A Novel Approach to Guidance and Control System Design Using Genetic-Based Fuzzy Logic Model

Chun-Liang Lin and Rei-Min Lai

***Abstract*—The proportional navigation guidance law usually guides traditional aerodynamically controlled missiles in the terminal phase. Such design approaches possess little flexibility on the improvement of engagement performance robustness. The Takagi–Sugeno (T–S) fuzzy logic theory and the gain scheduling technique are presented to design guidance and control (GC) parameters over coupled flight conditions. A genetic algorithm also serves as the computing device to determine the consequent function parameters of the fuzzy rules. The proposed design paradigm offers a way to implement simple but robust solutions that cover a wide range of aerodynamic variations. Complete simulation results illustrate the engagement performance and applicability of this design.**

***Index Terms*—Fuzzy logic applications, genetic algorithm (GA), guidance and control (GC), missile.**

I. Introduction

THE performance of a tactically guided missile depends upon the design parameters for the guidance and control (GC) system, i.e., navigation gain, guidance time filter, and autopilot time constant. Normally, the initial version of a system specification is based on parameters developed during the concept exploration phase [1], [2]. Traditional GC parameter design, though robust, is generally not restricted to the most successful optimization algorithm in any particular domain [3], [4]. In general, it is difficult to determine these parameters via conventional optimization techniques. The reason is three fold. First, the design should guarantee engagement robustness over a wide range of aerodynamic variations. Second, the magnitude of the GC parameters is usually restricted to compensate for the stability problem caused by the missile radome refraction slope errors. Third, the magnitude of these parameters should be strictly limited due to practical constraints.

For tactically guided missiles, the GC parameters are usually gain scheduled. They are switched along the flight trajectories according to a function or a table lookup with the scheduling variables. It is normally used in the control of nonlinear flight dynamics where the relationship between the plant dynamics and operating conditions is known, and for which a single linear time-invariant (LTI) model is insufficient. While a large number of papers have focused on missile autopilot design (see, for examples, [5], [6]), only a few results have been published with regard to the integrated GC system design [7]. The main drawback of most conventional gain scheduling (CGS) methods is that the parameter change may be rather abrupt across the region boundaries, which may result in unacceptable or even unstable performance [8]. Another problem is that accurate LTIs at various operating points may be difficult or impossible to obtain.

As a solution to this problem, a fuzzy gain scheduling (FGS) method has been proposed by Takagi and Sugeno (T–S) [9] that utilizes a fuzzy reasoning technique to determine the gain-scheduled parameters. With this method, human expertise in the linear control design and CGS can be represented by fuzzy rules with a fuzzy inference mechanism interpolating the controller parameters in the transition regions. For control and optimization purposes, it possesses two advantages over the traditional fuzzy inferencing mechanism.

1) The consequent of the rules are functions of the input variables. The defuzzification process is faster than the fuzzy inferencing systems; therefore, it is more appropriate for real-time applications.
2) The T–S FGS optimization involves only parametric learning (i.e., membership function and consequent function parameters) whereas the fuzzy inferencing systems require two optimization processes: parametric learning and structural learning.

For traditional fuzzy inferencing systems, a rule base is obtained from a human expert and the membership function is adjusted using trial and error. T–S FGS usually has more adjustable parameters in the rule consequent. Therefore, manual tuning of these parameters could be ineffective, or sometimes impossible when there are many parameters to adjust. This is partially due to the lack of intuitiveness in the T–S rule consequent. Recently, genetic algorithms (GAs) have been used as a tool to determine fuzzy membership functions or tune the output variable parameters of the T–S rule consequent [10]–[12]. GAs are stochastic optimization algorithms that were originally motivated by the natural selection mechanism and evolutionary genetics [13]. They simultaneously evaluate many points in the parameter space (called search space) and thus have a reduced chance of converging to the local optimum. This technique has also been applied to autopilot designs [14], [15]. However, a GA-based design for the missile guidance law is still lacking.

This paper proposes a systematic design methodology for designing the principal parameters of the GC system during the preliminary concept design phase. This novel design approach uses a T–S fuzzy system to represent the fuzzy relationship between the scheduling variables and the GC parameters. While three scheduling variables are defined by speed, altitude, and missile-target relative distance, it is shown that the com-

Manuscript received January 3, 2001; revised September 11, 2001. Manuscript received in final form November 21, 2001. Recommended by Associate Editor D. W. Repperger. This work was supported by National Science Council, Taiwan, R.O.C., under Grant NSC 89-2218-E-035-010.

The authors are with the Institute of Automatic Control Engineering, Feng Chia University, Taichung, Taiwan 40724, R.O.C. (e-mail: chunlin@fcu.edu.tw).

Publisher Item Identifier S 1063-6536(02)01765-7.

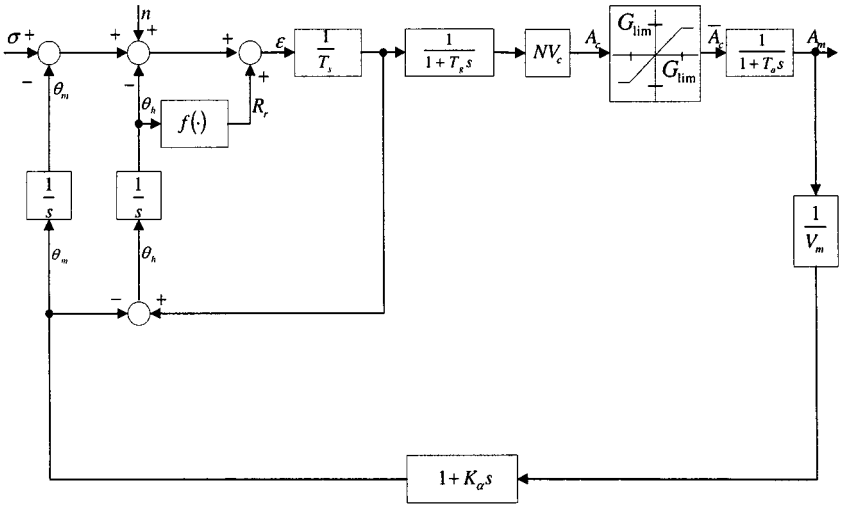

Fig. 1. Simplified missile guidance and control system.

plicated three-dimensional (3-D) fuzzy rule base can be simplified into an easily designed two-dimensional (2-D) rule base. Determining the consequent function parameters of the T–S FGS model is formulated as a complex constrained optimization problem. It is demonstrated that GA optimization technique can be successfully applied to enhance the system performance by incorporating several performance goals and constraints. Complete simulation studies show that the proposed design offers satisfactory endgame performance, and, in addition, a robustness feature to the aerodynamic variations.

II. GC System Descriptions

In preliminary missile GC system design, it is important to have a simplified system model to produce a performance evaluation that is meaningful but not overly optimistic. Fig. 1 shows the functional relationship between the major subsystems that contribute to guided missiles. In this figure, n is the total external noise (including receiver, glint, and servo noises), T_s is the seeker tracking loop time constant, N is the proportional navigation gain, V_c is the missile-target closing velocity, T_g is the guidance filter time constant, T_a is the flight control system (autopilot) time constant, K_α is the aerodynamic turning rate time constant, V_m is the missile velocity, σ is the line-of-sight (LOS) angle rate between the missile and target, ε is the boresight error (BSE) angle, θ_h is the gimbal angle radome refraction error $r = f(\theta_h)$, θ_m is the missile body angle, A_c is the acceleration command, $\overline{A}_c$ is the acceleration command saturation used to prevent both angle-of-attack saturation and airframe structural failure, A_m is the missile lateral acceleration, and A_t is the target evasive acceleration. Developing a simplified tracking and stabilization control system completes the seeker model. The radome refraction slope error [3] is approximated by $f(\theta_h) = RR_l\theta_h$ where RR_l denotes the equivalent radome refraction slope. For the terminal intercept (homing loop) simulation shown in Fig. 2, *RMT* indicates the relative range between missile and target. The final miss distance is denoted by $\mathrm{MD} = e(t_f)$ where t_f is the flight time. A band-limited Gaussian noise model is used to generate the target acceleration A_t.

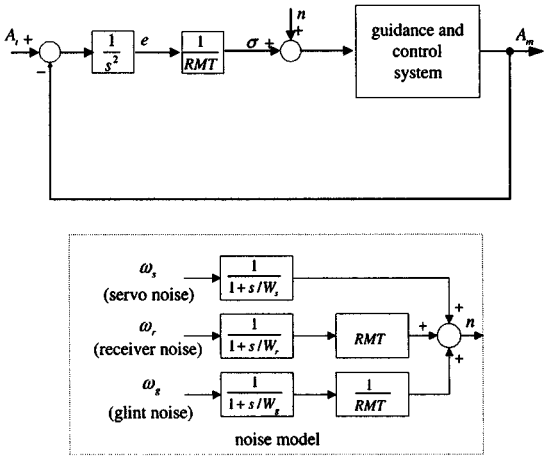

Fig. 2. Simplified homing loop.

By making use of the block diagram reduction technique, the diagram in Fig. 1 can be simplified to Fig. 3, in which

$$G_1(s) = \frac{T_g T_a s^2 + (T_g + T_a - K_\alpha N')s + 1 - N'}{(1+T_s s)(1+T_g s)(1+T_a s)}$$

$$G_2(s) = \frac{sNV_c}{(1+T_s s)(1+T_g s)(1+T_a s)}$$

with $N' = (NV_c/V_m)$. Since $G_2(s)$ is stable in the nominal GC system design, the inherent stability is determined by the dynamics between σ and $\tilde{\varepsilon} = \sigma + f(\theta_h)$ alone. Ignoring the external noise n, it can be shown that

$$\frac{\tilde{\varepsilon}(s)}{\sigma(s)} = \frac{[1 + (T_s + T_g + T_a)s]\beta^{-1}}{1 + \beta^{-1}(T_s + T_g + T_a + T_{\mathrm{par}})s} \tag{1}$$

for the situation of $|RR_l| \ll 1$, where $\tilde{\varepsilon} = \sigma + f(\theta_h)$, $\beta = 1 + N'RR_l$, the term $T_{\mathrm{par}} = RR_l N' K_\alpha$ denotes the parasitized time constant. In general, $|RR_l| < 0.05$, $N \le 5$ and $V_c/V_m \le 2$ for tactical guided missiles, the overall time constant T_{all} for the GC system can thus be approximated as

$$T_{\mathrm{all}} \approx T_s + T_g + T_a + T_{\mathrm{par}}. \tag{2}$$

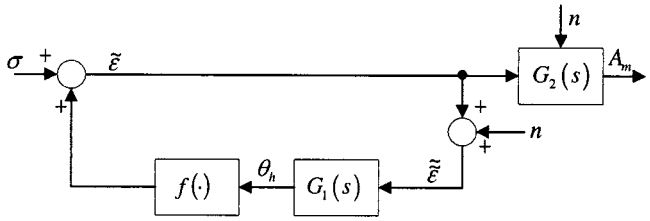

Fig. 3. Feedback connection used for stability evaluation.

The system is internally stable only if

$$T_{\text{all}} > 0. \tag{3}$$

Obviously, this holds naturally for $RR_l > 0$. On the other hand, for $RR_l < 0$, the internal stability condition becomes

$$T_s + T_g + T_a + \frac{RR_l N V_c K_\alpha}{V_m} > 0. \tag{4}$$

The effect of a positive RR_l is to increase T_{all}, thereby increasing MD due to target manuevers. If the radome refraction error is sufficiently large for a negative RR_l, T_{all} may lead to negative values resulting in an unstable system. The turning rate time constant K_α increases for high-altitude engagement. For those cases, the permissible range of the refraction slope decreases. On the other hand, K_α reduces with lower altitude. As a result, the permissible range of RR_l increases for low altitude engagement. Given the variations in K_α with the missile's altitude and speed, the major GC paramters N, T_g, and T_a are generally changed with the aerodynamic variation to maintain stability and best engagement performance.

In addition to the stability constraint, the parameters N, T_g and T_a should be strictly limited to avoid overriding the flight control system and hence cause damage to the actuating devices. Their reliable values are generally restricted in the following parameter space:

$$\Theta \equiv \{N, T_g, T_a \in \Re | (N, T_g, T_a) \text{ satisfies (3) and } \underline{N} \le N \le \overline{N},\ \underline{T}_g \le T_g \le \overline{T}_g,\ \underline{T}_a \le T_a \le \overline{T}_a\} \tag{5}$$

where $\underline{N}$, $\underline{T}_g$, and $\underline{T}_a$ indicate the prespecified lower bounds and $\overline{N}$, $\overline{T}_g$, and $\overline{T}_a$indicate the upper bounds.

III. T–S Fuzzy Logic GC System

The development of appropriate GC specifications is crucial to the performance of a guided missile. It is quite often either difficult to find or too complicated to determine the GC parameters. Fortunately, this can be partly resolved using the T–S fuzzy inference technique [9]. In the proposed design, the scheduling variables are taken as V_m, H_m, and *RMT*. The inference engine generates N, T_g, and T_a. *RMT* is determined by $V_c T_{\text{go}}$ where $T_{\text{go}} = t_f - t$ is the time to go. T_{go} is used to optimize the tradeoff between engagement performance and homing loop stability. When T_{go} is large, N should be small and the filtering (T_g and T_a) should be heavy enough to reduce the general motion due to large random accelerations responding to the noise. Yet N should be large and the filtering must be light enough to allow quick missile response when T_{go} is small to allow chasing a maneuvering target.

TABLE I
Twelve Flight Conditions and the Corresponding Aerodynamic Turning Rate Constants $K_\alpha(s)$

H_m(km) \ V_m(Mach)	1.6	1.8	2.0	2.2	2.4
17.5	FC(5,1) K_α = 3.0	FC(5,2) K_α = 2.9	FC(5,3) K_α = 2.8	FC(5,4) K_α = 2.7	FC(5,5) K_α = 2.6
15.0	FC(4,1) K_α = 2.5	FC(4,2) K_α = 2.4	FC(4,3) K_α = 2.3	FC(4,4) K_α = 2.2	FC(4,5) K_α = 2.1
12.5	FC(3,1) K_α = 2.0	FC(3,2) K_α = 1.9	FC(3,3) K_α = 1.8	FC(3,4) K_α = 1.7	FC(3,5) K_α = 1.6
10.0	FC(2,1) K_α = 1.5	FC(2,2) K_α = 1.4	FC(2,3) K_α = 1.3	FC(2,4) K_α = 1.2	FC(2,5) K_α = 1.1
7.5	FC(1,1) K_α = 1.0	FC(1,2) K_α = 0.9	FC(1,3) K_α = 0.8	FC(1,4) K_α = 0.7	FC(1,5) K_α = 0.6

A. T–S Fuzzy Rules

The standard form of the T–S fuzzy rules are described as follows:

$$\begin{aligned} R^{(1)}&\text{: if } x_1 \text{ is } LX_1^{(1)} \text{ and } \ldots \text{ and } x_n \text{ is } LX_n^{(1)} \\ &\quad \text{then } u_1 = f_1(x_1, \ldots, x_n) \\ &\quad \vdots \\ R^{(m)}&\text{: if } x_1 \text{ is } LX_1^{(m)} \text{ and } \ldots \text{ and } x_n \text{ is } LX_n^{(m)} \\ &\quad \text{then } u_m = f_m(x_1, \ldots, x_n) \end{aligned} \tag{6}$$

where $R^{(i)}$ denotes the ith control rule, $LX_j^{(i)}$ denotes the fuzzy set of the ith rule defined on x_j, u_i is the output which is the analytical function $f_i(\cdot)$ of the input variables. For given input values of the process variables $x_1^*, \ldots, x_n^*$, their degrees of membership $\mu_{LX_j^{(i)}}$, $j = 1, \ldots, n$ called rule-antecedent weights are calculated. The centroid defuzzifier evaluates the output of all rules as follows [9]:

$$u_c = \frac{\sum_{i=1}^{m} \mu_{u_i} u_i^*}{\sum_{i=1}^{m} \mu_{u_i}} \tag{7}$$

where $\mu_{u_i} = \min\left(\mu_{LX_1^{(i)}}(x_1^*), \ldots, \mu_{LX_n^{(i)}}(x_n^*)\right)$ or $\mu_{u_i} = \mu_{LX_1^{(i)}}(x_1^*) \cdots \mu_{LX_n^{(i)}}(x_n^*)$.

In the presented design we let the scheduling variables belong to the following universes of discourses: $x_1 \equiv V_m \in [\underline{V}_m, \overline{V}_m]$, $x_2 \equiv H_m \in [\underline{H}_m, \overline{H}_m]$ and $x_3 \equiv RMT \in [\underline{RMT}, \overline{RMT}]$. For the output variables, let $N \in [\underline{N}, \overline{N}]$, $T_g \in [\underline{T}_g, \overline{T}_g]$ and $T_a \in [\underline{T}_a, \overline{T}_a]$.

Twenty-five flight conditions under consideration with the corresponding aerodynamic turning rate constants K_α are given in Table I. The corresponding linguistic values, taken by the input scheduling variables, are expressed by linguistic sets. Each

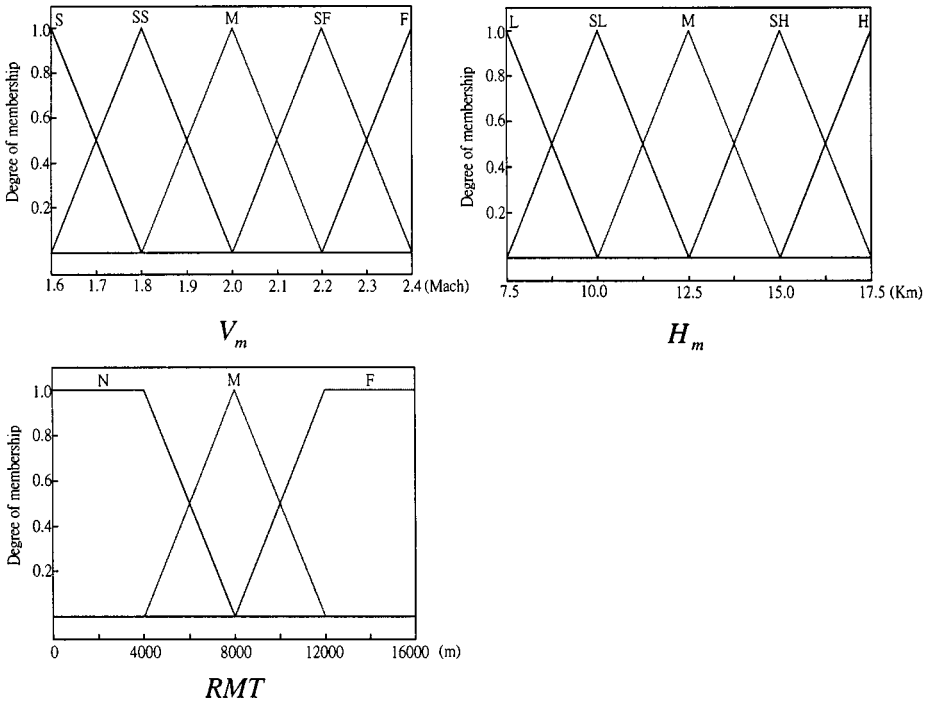

Fig. 4. Term sets of V_m, H_m, and *RMT* on specified domains.

N		V_m				
		S	*SS*	*M*	*SR*	*R*
H_m	*H*	M	SS	SS	S	S
	SH	M	SS	SS	S	S
	M	SL	M	M	SS	SS
	SL	SL	SL	M	M	SS
	L	L	SL	SL	M	M

T_g		V_m				
		S	*SS*	*M*	*SR*	*R*
H_m	*H*	L	L	SL	SL	M
	SH	L	L	SL	SL	M
	M	SL	SL	M	M	SS
	SL	SL	M	M	SS	SS
	L	M	M	SS	SS	S

T_a		V_m				
		S	*SS*	*M*	*SR*	*R*
H_m	*H*	L	L	SL	SL	M
	SH	L	L	SL	SL	M
	M	SL	SL	M	M	SS
	SL	SL	M	M	SS	SS
	L	M	M	SS	SS	S

Fig. 5. Prototype rule base for "*RMT* is M."

of the scheduling variables is assumed to take the following term sets:

$$T_{V_m} = \{LX_{11}, LX_{12}, LX_{13}, LX_{14}, LX_{15}\} = \{\mathrm{S}, \mathrm{SS}, \mathrm{M}, \mathrm{SR}, \mathrm{R}\} \quad (8a)$$

$$T_{H_m} = \{LX_{21}, LX_{22}, LX_{23}, LX_{24}, LX_{25}\} = \{\mathrm{L}, \mathrm{SL}, \mathrm{M}, \mathrm{SH}, \mathrm{H}\} \quad (8b)$$

$$T_{RMT} = \{LX_{31}, LX_{32}, LX_{33}\} = \{\mathrm{N}, \mathrm{M}, \mathrm{F}\} \quad (8c)$$

where the fuzzy sets: S $\equiv$ Slow, SS $\equiv$ Slightly Slow, M $\equiv$ Medium, SR $\equiv$ Slightly Rapid, R $\equiv$ Rapid, L $\equiv$ Low, SL $\equiv$ Slightly Low, SH $\equiv$ Slightly High, H $\equiv$ High, N $\equiv$ Near, F $\equiv$ Far. These linguistic sets are described by their membership functions, shown in Fig. 4, where for the simulation studies purposes, we have set $\underline{V}_m = 1.6$ Mach, $\overline{V}_m = 2.4$ Mach, $\underline{H}_m = 7.5$ km, $\overline{H}_m = 17.5$ km, and $\underline{RMT} = 0.0$ km, $\overline{RMT} = 16.0$ km.

The complete rule base should contain $m = 5 \times 5 \times 3$ fuzzy rules. The term sets of the consequent part consist of

$$T_N = \{N_1, \ldots, N_m\}, \quad T_{T_g} = \{T_{g1}, \ldots, T_{gm}\}$$
$$T_{T_a} = \{T_{a1}, \ldots, T_{am}\}$$

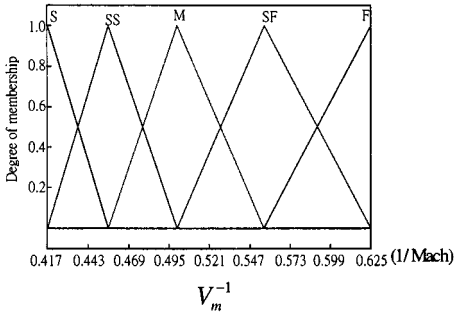

Fig. 6. Term set of V_m^{-1}.

N		$1/V_m$				
		S	*SS*	*M*	*SR*	*R*
H_m	*H*	S	S	SS	SS	M
	SH	S	S	SS	SS	M
	M	SS	SS	M	M	SL
	SL	SS	M	M	SL	SL
	L	M	M	SL	SL	L

Fig. 7. Modified rule base for the navigation gain N.

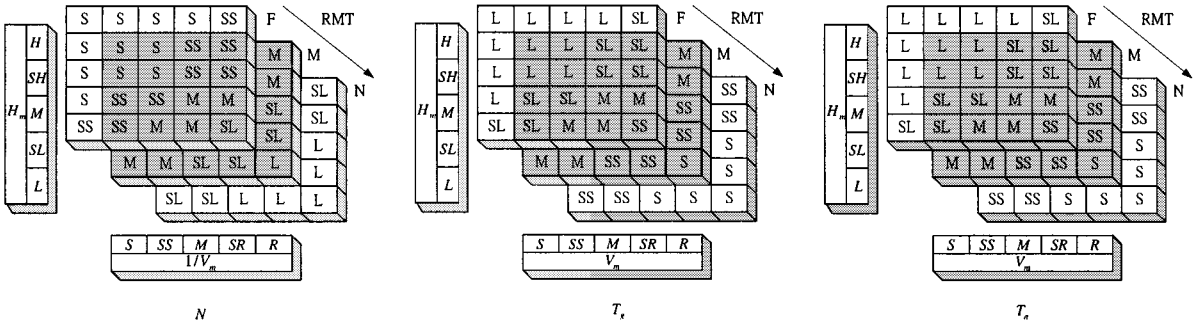

Fig. 8. Proposed fuzzy rule bases for the GC parameters.

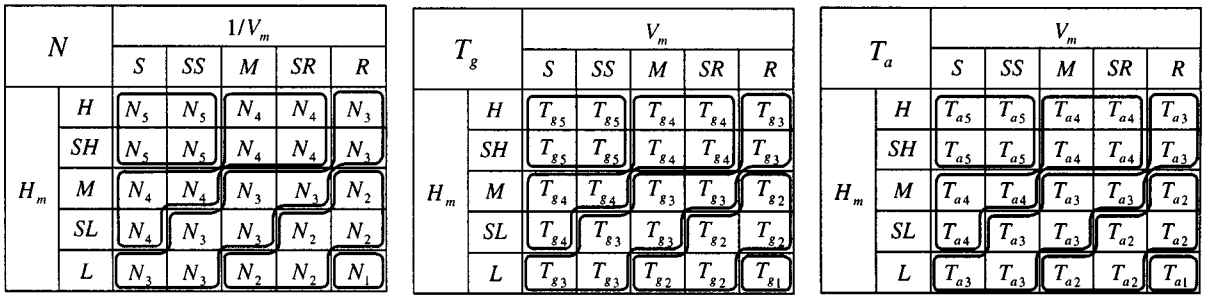

Fig. 9. TS-type fuzzy rule base for "*RMT* is M."

where the scheduled GC parameters are defined by

$$\begin{aligned} N_i =& \alpha_1^{(i)} V_m + \beta_1^{(i)} H_m + \gamma_1^{(i)} T_{\text{go}} \\ T_{gi} =& \alpha_2^{(i)} V_m + \beta_2^{(i)} H_m + \gamma_2^{(i)} T_{\text{go}}, \quad i = 1, \ldots, m \\ T_{ai} =& \alpha_3^{(i)} V_m + \beta_3^{(i)} H_m + \gamma_3^{(i)} T_{\text{go}}. \end{aligned} \tag{9}$$

In this expression, the consequent function parameters of the fuzzy rules α_i, β_i, and γ_i can be viewed as the weighting factors for the variables V_m, H_m, and T_{go}, respectively.

It can be seen from Fig. 4 that the fuzzy sets of the antecedent part satisfy

$$\begin{aligned} \mu_{LX_{ij}}(x_i) + \mu_{LX_{i(j+1)}}(x_i) =& 1, \ \forall x_i \in \left[x_{ij},\, x_{i(j+1)}\right] \\ & i = 1, 2, \ j = 1, \ldots, 4 \end{aligned} \tag{10a}$$

$$\begin{aligned} \mu_{LX_{3j}}(x_3) + \mu_{LX_{3(j+1)}}(x_3) =& 1, \ \forall x_3 \in \left[x_{3j}, x_{3(j+1)}\right] \\ & j = 1, 2. \end{aligned} \tag{10b}$$

Based on these properties, we used product-sum inference to speed up computation in finding the GC parameters. When the crisp inputs at the time t are x_1^*, x_2^*, and x_3^*, we get three tuples (μ_{N_i}, N_i^*), $\left(\mu_{T_{g_i}}, T_{g_i}^*\right)$ and $\left(\mu_{T_{a_i}}, T_{a_i}^*\right)$ of the ith rule with the rule-antecedent weights defined by

$$\begin{aligned} \mu_{N_i} =& \mu_{LX_1^{(i)}}(x_1^*)\, \mu_{LX_2^{(i)}}(x_2^*)\, \mu_{LX_3^{(i)}}(x_3^*) \\ \mu_{T_{g_i}} =& \mu_{LX_1^{(i)}}(x_1^*)\, \mu_{LX_2^{(i)}}(x_2^*)\, \mu_{LX_3^{(i)}}(x_3^*) \\ \mu_{T_{a_i}} =& \mu_{LX_1^{(i)}}(x_1^*)\, \mu_{LX_2^{(i)}}(x_2^*)\, \mu_{LX_3^{(i)}}(x_3^*). \end{aligned}$$

From (10), for $x_1^* \in [x_{1i}, x_{1(i+1)}]$, $x_2^* \in [x_{2j}, x_{2(j+1)}]$, and $x_3^* \in [x_{3k}, x_{3(k+1)}]$, we get

$$\begin{aligned} \sum_{i=1}^{m} \mu_N =& \sum_{t=k}^{k+1} \sum_{s=j}^{j+1} \sum_{r=i}^{i+1} \mu_{LX_{1r}}(x_1^*)\, \mu_{LX_{2s}}(x_2^*)\, \mu_{LX_{3t}}(x_3^*) \\ =& \left(\mu_{LX_{1i}}(x_1^*) + \mu_{LX_{1(i+1)}}(x_1^*)\right) \\ & \times \left(\mu_{LX_{2j}}(x_2^*) + \mu_{LX_{2(j+1)}}(x_2^*)\right) \\ & \times \left(\mu_{LX_{3k}}(x_3^*) + \mu_{LX_{3(k-1)}}(x_3^*)\right) \\ =& 1. \end{aligned} \tag{11a}$$

Similarly, we have

$$\begin{aligned} \sum_{p=1}^{m} \mu_{T_{g_p}} =& \sum_{t=k}^{k+1} \sum_{s=j}^{j+1} \sum_{r=i}^{i+1} \mu_{LX_{1r}}(x_1^*)\, \mu_{LX_{2s}}(x_2^*)\, \mu_{LX_{3t}}(x_3^*) \\ =& 1 \\ \sum_{p=1}^{m} \mu_{T_{a_p}} =& \sum_{t=k}^{k+1} \sum_{s=j}^{j+1} \sum_{r=i}^{i+1} \mu_{LX_{1r}}(x_1^*)\, \mu_{LX_{2s}}(x_2^*)\, \mu_{LX_{3t}}(x_3^*) \\ =& 1. \end{aligned} \tag{11b}$$

Therefore, using (7) and (11) and the rule consequent given in (9) the crisp GC parameters are obtained as

$$\begin{aligned} N =& \sum_{p=1}^{m} \mu_{N_p} N_p^* \\ =& \sum_{t=k}^{k+1} \sum_{s=j}^{j+1} \sum_{r=i}^{i+1} \mu_{LX_{1r}}(x_1^*)\, \mu_{LX_{2s}}(x_2^*)\, \mu_{LX_{3t}} \\ & \times (x_3^*) \left(\alpha_1^{(rst)} x_1^* + \beta_1^{(rst)} x_2^* + \gamma_1^{(rst)} \frac{1}{V_c} x_3^*\right) \end{aligned}$$

$$
\begin{aligned}
T_g &= \sum_{p=1}^{m} \mu_{T_{g_p}} T_{g_p}^* \\
&= \sum_{t=k}^{k+1} \sum_{s=j}^{j+1} \sum_{r=i}^{i+1} \mu_{LX_{1r}}(x_1^*)\, \mu_{LX_{2s}}(x_2^*)\, \mu_{LX_{3t}} \\
&\quad \times (x_3^*) \left(\alpha_2^{(rst)} x_1^* + \beta_2^{(rst)} x_2^* + \gamma_2^{(rst)} \frac{1}{V_c} x_3^* \right) \\
T_a &= \sum_{p=1}^{m} \mu_{T_{ap}} T_{a_p}^* \\
&= \sum_{t=k}^{k+1} \sum_{s=j}^{j+1} \sum_{r=i}^{i+1} \mu_{LX_{1r}}(x_1^*)\, \mu_{LX_{2s}}(x_2^*)\, \mu_{LX_{3t}} \\
&\quad \times (x_3^*) \left(\alpha_3^{(rst)} x_1^* + \beta_3^{(rst)} x_2^* + \gamma_3^{(rst)} \frac{1}{V_c} x_3^* \right) \quad (12)
\end{aligned}
$$

where $\alpha^{(rst)}$, $\beta^{(rst)}$, and $\gamma^{(rst)}$ represent, respectively, the weighting factors for x_1^*, x_2^*, and x_3^*.

B. Construction of Fuzzy Rule Base

Due to the lack of intuitiveness of the T–S rule consequent, how to determine $25 \times 3 \times 3$ consequent function parameters becomes a difficult problem. To overcome this, a traditional fuzzy rule base in a table format is constructed first. The complete rule base describing the GC parameters contains $5 \times 5 \times 3$ rules. To simplify the parameter design work, only the situation of "*RMT* is M" is preliminarily considered. Once the design is completed, it is directly extended to the situations of "*RMT* is N" and "*RMT* is F" with minor modifications.

Based on the following guidelines, a rule prototype shown in Fig. 5 is constructed.

1) Due to larger aerodynamic turning rate time constant, the navigation gain tends to decrease and the guidance filter and autopilot time constants tend to increase at higher altitudes so that the stability requirement caused by negative radome errors can be maintained.
2) At the same altitude, larger navigation gains and lighter time constants from the guidance filter and autopilot tend to enhance missile response at lower speeds. In addition, the filtering must be light enough to allow quick missile response when corrections are needed for heading errors or to chase a maneuvering target.

The term set describing the GC parameters N, T_g, and T_a consists of five fuzzy sets: {S, SS, M, SL, L} where S ≡ Small, SS ≡ Slightly Small, M ≡ Medium, SL ≡ Slightly large, and L ≡ Large.

While the term set for N consists of the same fuzzy sets as those for T_g and T_a, as seen from Fig. 5, the distribution of their rule bases are quite different. For design convenience, the scheduling variable V_m determining for N is transformed into V_m^{-1} and its corresponding membership functions is shown in Fig. 6. Using this transformation, the ruble base of Fig. 5(a) can be transformed into the rule base shown in Fig. 7. Clearly, the rule bases for N, T_g, and T_a now possess a consistent grouping for the rule consequent. Each group of fuzzy rules shown in Figs. 5(b), 5(c), and 7 possesses the same antecedent fuzzy sets as well as the same number of consequent fuzzy sets.

To fully exploit the maneuvering capability of the missile, it is appropriate to use a larger navigation ratio and lighter time constant for the guidance filter and autopilot when *RMT* gradually approaches zero. Based on this criterion, the rule bases for "*RMT* is N" and "*RMT* is F" can be obtained by simply modifying the one for "*RMT* is M." For "*RMT* is F," we create a "rule window" over the original rule table (referring to Fig. 8) of "*RMT* is M," in which the rule for $\left(H_m, V_m^{-1}\right) = (L, R)$ is "N is *SL*," which remains the same inference with that of "*RMT* is M" at $\left(H_m, V_m^{-1}\right) = (SL, SR)$. The rule for $\left(H_m, V_m^{-1}\right) = (SH, SS)$ is "N is S," which remains the same inference as "*RMT* is M" at $\left(H_m, V_m^{-1}\right) = (S, H)$, etc. The rules for "$H_m$ is H" and "V_m^{-1} is S" are then attached to complete the table. Similar treatment also applies to "*RMT* is N." This greatly simplifies the work from designing a complicated, 3-D rule base to an easily designed 2-D one.

TABLE II
HOMING LOOP PARAMETERS

Notation	Nominal Value
Seeker tracking loop time constant T_s	0.1s
Torque servo gain K_s	100rad/s
Acceleration command limit $G_{\lim}$	15.0g (g=9.8m/s^2)
Radome refraction slope RR_l	-0.03rad/rad
Target velocity V_t	400.0m/s
Initial relative range $RMT\big\|_{t=0}$	10000.0m
MD specification ε_{md}	3.6m

We have built antecedent membership functions and appropriate consequent functions for the FGS rules using human expertise. However, the inferenced parameters may not be the optimum. Furthermore, calculation of the defuzzification is time consuming. The standard fuzzy rule base is thus converted into the T–S type rule base shown as in Fig. 9 (for brevity only the case that "*RMT* is M" is shown). The consequent navigation gains $(N_1, N_2, N_3, N_4, N_5)$ in Fig. 9(a) correspond to the fuzzy sets (L, SL, M, SS, S) in Fig. 8(a). The consequent guidance filter time constants $(T_{g1}, T_{g2}, T_{g3}, T_{g4}, T_{g5})$ in Fig. 9(b) corresponds to the fuzzy sets (S, SS, M, SL, L) in Fig. 8(b) and the consequent autopilot time constant $(T_{a1}, T_{a2}, T_{a3}, T_{a4}, T_{a5})$ in Fig. 9(c) corresponds to the fuzzy sets (S, SS, M, SL, L) in Fig. 8(c). The T–S type rule bases for "*RMT* is N" and "*RMT* is F" are constructed by the same way. Using (12), the GC parameters can be expressed in terms of the scheduling variables

$$
\begin{aligned}
N_p &= \sum_{t=k}^{k+1} \sum_{s=j}^{j+1} \sum_{r=i}^{i+1} \mu_{LX_{1r}}\left(V_m^{-1^*}\right) \mu_{LX_{2s}}(H_m^*)\, \mu_{LX_{3t}} \\
&\quad \times (RMT^*) \left(\alpha_1^{(rst)} V_m^{-1^*} + \beta_1^{(rst)} H_m^* + \gamma_1^{(rst)} T_{\mathrm{go}}^* \right) \\
T_{gp} &= \sum_{t=k}^{k+1} \sum_{s=j}^{j+1} \sum_{r=i}^{i+1} \mu_{LX_{1r}}(V_m^*)\, \mu_{LX_{2s}}(H_m^*)\, \mu_{LX_{3t}}(RMT^*) \\
&\quad \times \left(\alpha_2^{(rst)} V_m^* + \beta_2^{(rst)} H_m^* + \gamma_2^{(rst)} T_{\mathrm{go}}^* \right) \\
p &= 1, \ldots, 5 \\
T_{ap} &= \sum_{t=k}^{k+1} \sum_{s=j}^{j+1} \sum_{r=i}^{i+1} \mu_{LX_{1r}}(V_m^*)\, \mu_{LX_{2s}}(H_m^*)\, \mu_{LX_{3t}}(RMT^*) \\
&\quad \times \left(\alpha_3^{(rst)} V_m^* + \beta_3^{(rst)} H_m^* + \gamma_3^{(rst)} T_{\mathrm{go}}^* \right). \quad (13)
\end{aligned}
$$

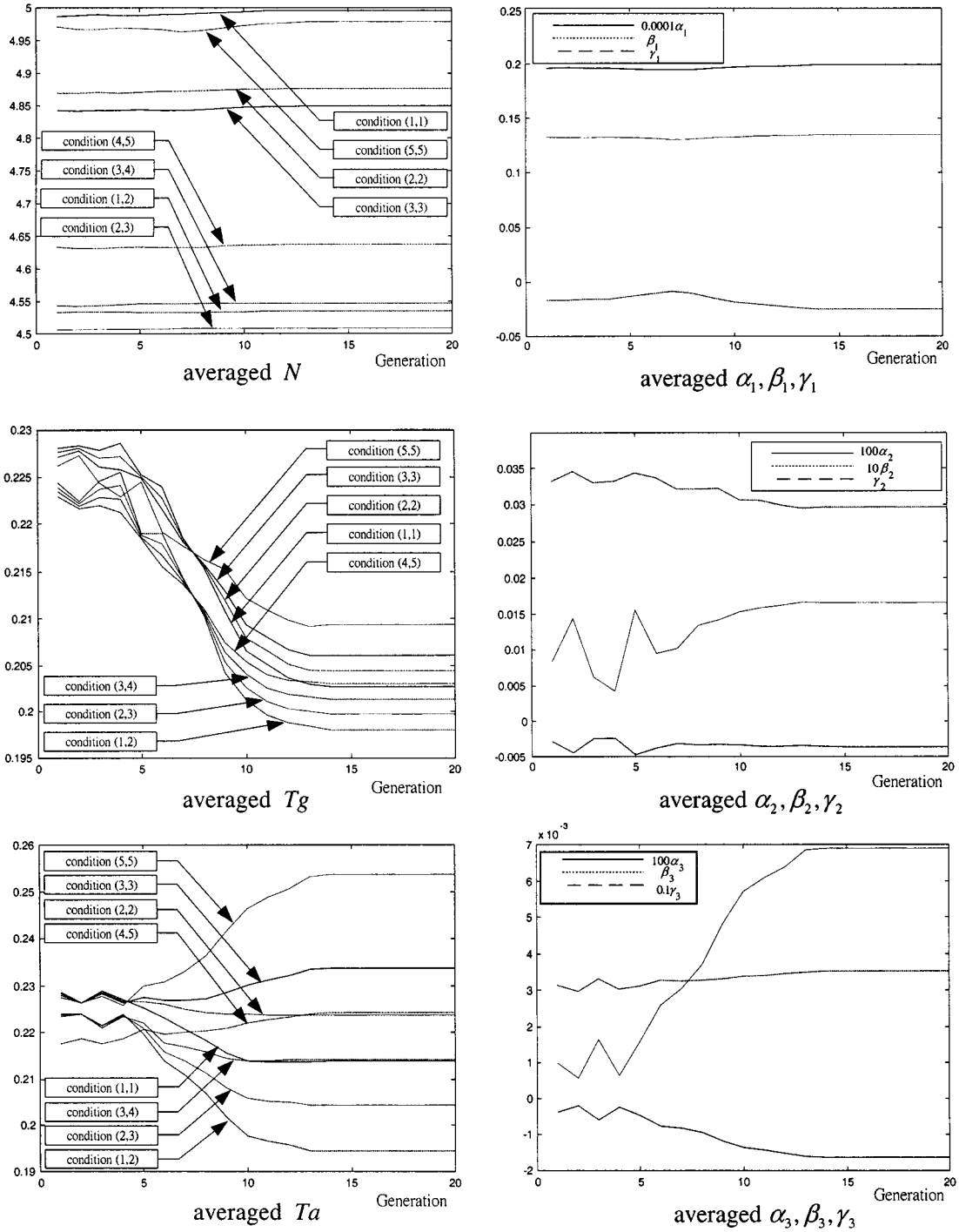

Fig. 10. Convergence of GC parameters.

N_i, T_{g_i}, and T_{a_i} are packed into five groups, denoted by P_1–P_5, and the ranges for the elements in each group are specified as follows:

$$P_i \equiv \left\{N_i \in \left[\underline{N}_i, \overline{N}_i\right], T_{g_i} \in \left[\underline{T}_{g_i}, \overline{T}_{g_i}\right], T_{ai} \in \left[\underline{T}_{a_i}, \overline{T}_{a_i}\right]\right\} \quad i = 1, \ldots, 5. \tag{14}$$

The problem is now shifted to determine the appropriate consequent function parameters $\alpha_j^{(i)}$, $\beta_j^{(i)}$, and $\gamma_j^{(i)}$, $\forall\, i, j$ for the "*RMT* is M" situation.

IV. Consequent Function Parameter Design Using GAs

For the T–S fuzzy rule table, 45 consequent function parameters fitting 25 flight conditions must be ultimately determined. It is either unrealistic or time consuming to directly search for the parameters using any parameter optimization technique. GAs have advantages in that the solution space is explored in parallel by searching different regions, thus they allow a global search in the solution space. Furthermore, the search mechanism is not based on gradient information and therefore has no requirements for continuity or convexity in the solution space.

TABLE III
CONSEQUENT FUNCTION PARAMETERS OF THE FUZZY RULE BASE

	N	T_g	T_a
P_1	$\alpha_1^{(1)} = 2.52\times10^{4}$	$\alpha_2^{(1)} = -1.93\times10^{-2}$	$\alpha_3^{(1)} = -2.64\times10^{-2}$
	$\beta_1^{(1)} = -3.28\times10^{0}$	$\beta_2^{(1)} = 1.02\times10^{0}$	$\beta_3^{(1)} = -6.53\times10^{-2}$
	$\gamma_1^{(1)} = -7.13\times10^{-1}$	$\gamma_2^{(1)} = 9.38\times10^{-1}$	$\gamma_3^{(1)} = 2.94\times10^{0}$
P_2	$\alpha_1^{(2)} = 3.09\times10^{3}$	$\alpha_2^{(2)} = -4.65\times10^{-4}$	$\alpha_3^{(2)} = 1.28\times10^{-4}$
	$\beta_1^{(2)} = 1.59\times10^{-1}$	$\beta_2^{(2)} = 2.59\times10^{-3}$	$\beta_3^{(2)} = -7.27\times10^{-3}$
	$\gamma_1^{(2)} = -1.28\times10^{-1}$	$\gamma_2^{(2)} = 6.57\times10^{-2}$	$\gamma_3^{(2)} = 1.83\times10^{-2}$
P_3	$\alpha_1^{(3)} = 1.99\times10^{3}$	$\alpha_2^{(3)} = -3.60\times10^{-5}$	$\alpha_3^{(3)} = -1.62\times10^{-4}$
	$\beta_1^{(3)} = 1.35\times10^{-1}$	$\beta_2^{(3)} = 1.66\times10^{-3}$	$\beta_3^{(3)} = 6.88\times10^{-3}$
	$\gamma_1^{(3)} = -2.51\times10^{-2}$	$\gamma_2^{(3)} = 2.97\times10^{-2}$	$\gamma_3^{(3)} = 3.50\times10^{-2}$
P_4	$\alpha_1^{(4)} = 1.62\times10^{3}$	$\alpha_2^{(4)} = -3.62\times10^{-4}$	$\alpha_3^{(4)} = 2.06\times10^{-4}$
	$\beta_1^{(4)} = 1.22\times10^{-1}$	$\beta_2^{(4)} = 4.78\times10^{-3}$	$\beta_3^{(4)} = -5.71\times10^{-3}$
	$\gamma_1^{(4)} = -6.25\times10^{-2}$	$\gamma_2^{(4)} = 6.59\times10^{-2}$	$\gamma_3^{(4)} = 4.19\times10^{-2}$
P_5	$\alpha_1^{(5)} = 1.84\times10^{3}$	$\alpha_2^{(5)} = -8.50\times10^{-5}$	$\alpha_3^{(5)} = -9.12\times10^{-4}$
	$\beta_1^{(5)} = 1.12\times10^{-2}$	$\beta_2^{(5)} = -1.82\times10^{-2}$	$\beta_3^{(5)} = 1.14\times10^{-3}$
	$\gamma_1^{(5)} = -5.13\times10^{-3}$	$\gamma_2^{(5)} = 1.05\times10^{-1}$	$\gamma_3^{(5)} = 1.21\times10^{-1}$

It is thus appropriate using a GA to determine the consequent function parameters in (13).

A GA is an iterative procedure that maintains a constant population size p_l of candidate solutions. In each generation, three basic genetic operators, i.e., reproduction, crossover, and mutation, are performed to generate a new population and the chromosomes of the population are evaluated via our proposed fitness functions. The GA elements that determine the GC parameters are summarized in the following.

1) *Coding and Decoding*: A binary GA works with a population of chromosomes or strings. In the proposed GA, the strings for the consequent function parameters expanded by $\left(\alpha_j^{(i)}, \beta_j^{(i)}, \gamma_j^{(i)}\right)$ are formed by concatenating substrings, each of which is a binary coding of a parameter of the search space expressed by

$$s_r = s_{r1} s_{r2} s_{r3} \tag{15}$$

where

$$s_{rj} = L_{\alpha_j^{(i)}1} L_{\alpha_j^{(i)}2} \cdots L_{\alpha_j^{(i)}n} L_{\beta_j^{(i)}1} L_{\beta_j^{(i)}2} \cdots L_{\beta_j^{(i)}m} L_{\gamma_j^{(i)}1} L_{\gamma_j^{(i)}2} \cdots L_{\gamma_j^{(i)}l}$$

and L_i is a variable taking a value of either "1" or "0." Using a binary coding method, every element θ_k of the parameter vector $\theta = \left[\alpha_j^{(i)} \quad \beta_j^{(i)} \quad \gamma_j^{(i)}\right]^T$ is coded as a string of l_k for the desired resolution R_k

$$R_k = \frac{\theta_{kh} - \theta_{kl}}{2^{l_k} - 1}$$

where θ_{kh} and θ_{kl} indicate the upper and lower limits of θ_k. A set of individuals S, called a population, is expressed as follows:

$$S = \{s_1, s_2, \ldots, s_m\}.$$

The decoding process is simply the inverse procedure to the coding process.

2) *Fitness*: Our ultimate objective is to search the consequent function parameters so that the resulting GC parameter set minimizes MD and avoids causing an impracticably large acceleration command over the homing phase due to target maneuvers. With regard to the engagement performance and control energy consumption, an appropriate cost function is set up as follows:

$$E(N_i, T_{g_i}, T_{a_i}) = \min_{N_i, T_{g_i}, T_{a_i} \in \Theta} \left[|MD| + \rho \int_0^{t_f} \left(\frac{A_c}{9.8}\right)^2 dt \right] \tag{16}$$

where A_c is in m/s^2 units, subject to the explicit performance constraint

$$|MD| \le \varepsilon_{md} \tag{17}$$

where ρ is a weighting factor included to permit adjustment of the relative importance of MD and total control energy consumption calculated over the homing phase and ε_{md} is the acceptable upper boundary of MD. The cost function is transformed into a fitness function $F(N_i, T_{g_i}, T_{a_i})$ so that the GA can be operated. Intuitively, we have

$$F(N_i, T_{g_i}, T_{a_i}) \propto \frac{1}{E(N_i, T_{g_i}, T_{a_i})}. \tag{18}$$

A linear equation can be introduced to connect E and F as follows:

$$F(N_i, T_{g_i}, T_{a_i}) = \lambda E(N_i, T_{g_i}, T_{a_i}) + \eta \tag{19}$$

where $\lambda = (F_u - F_l)/(E_l - E_u)$ and $\eta = F_u - \lambda E_l$ with the subscripts u and l indicating the largest and smallest values, respectively.

3) *Reproduction*: In this process, strings with high fitness receive multiple copies in the next generation while strings with low fitness receive fewer copies or even none at all. Here a chromosome from the current reproduction in each generation is reproduced into the next generation according to the reproduction probability p_{rk}

$$p_{rk} = \frac{F_k(N_i, T_{g_i}, T_{a_i})}{\sum_{k=1}^{p_l} F_k(N_i, T_{g_i}, T_{a_i})}. \tag{20}$$

Assigning more reproductive occurrences to above average individuals, the overall effect is to increase the population's average fitness.

4) *Crossover and Mutation*: Crossover exchanges the information of any two chromosomes to derive a new individual $s_r'(k)$ via probabilistic decision in a mating pool and provides a mechanism to mix and match desirable qualities through a random process. Two chromosomes in the mating pool are first selected randomly according to the crossover probability p_c. A splice point indicating the ith and $(i+1)$th bits of a string is determined uniformly at random. Finally, the genetic codes in front of the splice point are kept invariant, while the codes following the splice point are interchanged. Mutation is the random alteration of a bit in the string that assists in maintaining diversity in the population.

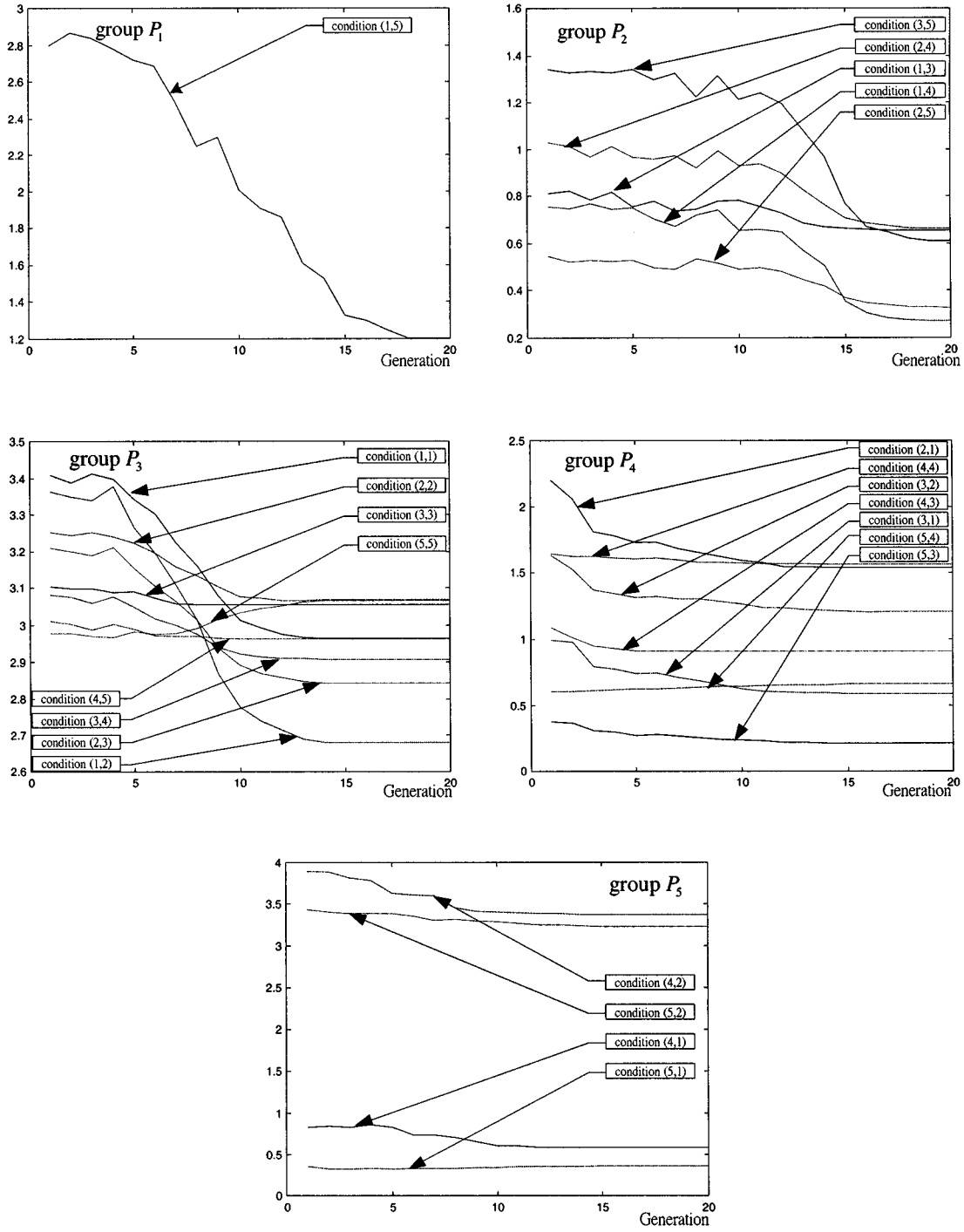

Fig. 11. Convergence of averaged values of cost functions.

It is an insurance strategy applied to each of the elements of individual $s'_r(k)$ according to the mutation probability p_m to ensure that all points in the search space can ultimately be researched. The dynamic parameters p_c and p_m defined below are used in the search operation

$$p_c,\, p_m = 1 - \left(\frac{SI}{AI}\right)^r, \quad 0 \le r \le 1 \tag{21}$$

where SI denotes the numbers of individuals satisfying the exceptional condition, AI denotes the number of all individuals. This provides faster convergence when compared to constant probability rate cases.

A. Design Process

Choose the appropriate genetic parameters p_c, p_m, p_l, and the desired resolution R. Flight conditions and the distributions of the GC parameters are partitioned according to Fig. 9. Determining the consequent function parameters can be outlined as follows.

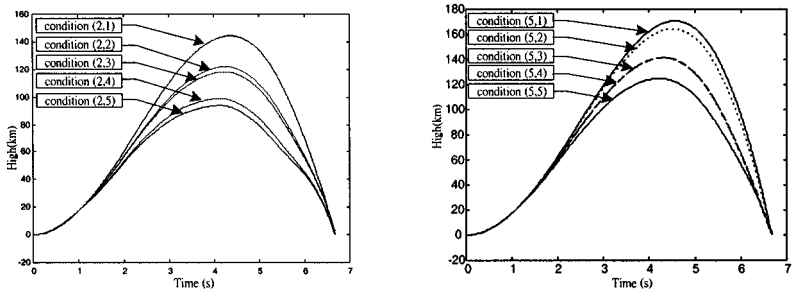

Fig. 12. Flight trajectories for designed flight conditions.

Step 1) Specify the GC parameter space Θ via (3). Additional constraints can also be imposed, if necessary.

Step 2) Randomly generate the consequent function parameters $\left(\alpha_j^{(i)}, \beta_j^{(i)}, \gamma_j^{(i)}\right)$ which contain the gene indexes that will be changed and based on the scheduling variables. Obtain the GC parameters via (13). The individuals $s_1, s_2, \ldots, s_m$ in the form of (15) will constitute the initial population. Elements of $S(0)$ are formulated using random binary strings.

Step 3) Decode the chromosomes into real parameters. Check if the GC parameters and $T_{\text{go}} \in [0, t_f]$ of the group P_i lie inside the permissible parameter space (5). If not, go to Step 2) until all corresponding GC parameters fall into Θ.

Step 4) Execute a couple of homing loop simulations (each case corresponding to a specific flight condition) within the prespecified group P_i to record the final MD and control energy consumption. Calculate the number of homing loop simulations for a population of chromosomes if those cases fail to meet the MD requirement (17).

Step 5) If the search goal or the prespecified number of generations is attained then stop. Otherwise, continue the steps.

Step 6) According to the number of individuals that satisfy (17) determine the appropriate mutation and crossover rates using (21).

Step 7) Calculate the required chromosome length.

Step 8) Encode $\left(\alpha_j^{(i)}, \beta_j^{(i)}, \gamma_j^{(i)}\right)$ into a binary string using (15).

Step 9) Create the offspring via reproduction, crossover, and mutation.

Step 10) Create a new generation. Steps 3)–8) are repeated until all individuals converge. An individual having the highest fitness in the converged population is chosen as the final solution.

V. Simulation Studies

This section presents simulation experiments to validate the proposed algorithm and investigate its behavior. The purpose is to present a robust GC parameter design and to maintain engagement performance over a wide range of aerodynamic variations. Nominal parameters used for the homing loop simulation are listed in Table II. For practical considerations, N, T_g, and T_a are restricted within the following parameter space:

$$\Theta \equiv \{N, T_g, T_a \in \Re | (N, T_g, T_a) \text{ satisfies (3) and } 3.5 \le N \le 6,\ 0.05 \le T_g \le 0.4,\ 0.05 \le T_a \le 0.4\}.$$

According to the rule base shown in Fig. 9, the consequent function parameters of the T–S type rule base are first partitioned into five groups

$$P_1 \equiv \{N_1 \in [5.5, 6.0],\ T_{g1} \in [0.05, 0.12],\ T_{a1} \in [0.05, 0.12]\}$$
$$P_2 \equiv \{N_2 \in [5.0, 5.5],\ T_{g2} \in [0.12, 0.19],\ T_{a2} \in [0.12, 0.19]\}$$
$$P_3 \equiv \{N_3 \in [4.5, 5.0],\ T_{g3} \in [0.19, 0.26],\ T_{a3} \in [0.19, 0.26]\}$$
$$P_4 \equiv \{N_4 \in [4.0, 4.5],\ T_{g4} \in [0.26, 0.33],\ T_{a4} \in [0.26, 0.33]\}$$
$$P_5 \equiv \{N_5 \in [3.5, 4.0],\ T_{g5} \in [0.33, 0.40],\ T_{a5} \in [0.33, 0.40]\}.$$

Let the resolution of $\alpha_j^{(i)}$, $\beta_j^{(i)}$, and $\gamma_j^{(i)}$ be slightly finer than 1.5×10^{-4} thus we need three binary string each with the length 11 to constitute θ_k. Initially, 300 combinations of $\alpha_j^{(i)}$, $\beta_j^{(i)}$, and $\gamma_j^{(i)}$ are randomly chosen. They are used to initialize the GC parameters N, T_g, and T_a.

Experience shows that care is needed in choosing the processing parameters p_l, p_c, and p_m to make the GAs work satisfactory. An appropriate choice of these parameters will speed up the convergence of the genetic search. Larger p_l and p_c usually result in fast convergence. Larger p_m may guarantee the search not to be trapped in a local minimum, however, the GA may tend toward a random search.

During the search, the length of the chromosome at each generation is adaptively controlled to reduce the computational effort while maintaining the accuracy of the search result. The GA parameters p_c and p_m are chosen according to (21). At the initial stage, they are set to be larger values to speed up the optimum seeking. After that they decrease gradually to avoid the GA with tendencies to overshoot. Fig. 10 displays the profiles of the averaged values for N, T_g, T_a, α, β, and γ after 20 generations of genetic search for the group P_3. Due to space limitations, only the results corresponding to group P_3 are provided. Table III lists the final consequent function parameters $\alpha_j^{(i)}$, $\beta_j^{(i)}$, and $\gamma_j^{(i)}$ searched by the proposed GA. Each tabular set of $\left(\alpha_j^{(i)}, \beta_j^{(i)}, \gamma_j^{(i)}\right)$ possesses the maximal fitness value over others in the population.

A. Performance Robustness Evaluation

The averaged values of cost functions calculated over 25 flight conditions with respect to 20 generations of chromo-

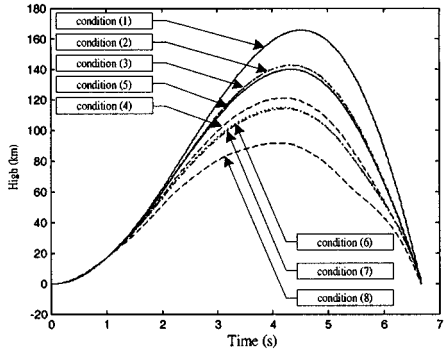

Fig. 13. Flight trajectories for off-designed flight conditions.

somes are illustrated in Fig. 11. It can be seen that the cost values converge after 15 generations of genetic evolution. Fig. 12 shows the MD trajectories for the guided missile under all flight conditions. The figure shows that the missile can effectively engage the target for all cases. It can be seen that there is no flight trajectory that presents a considerable variant from the others. These results demonstrate excellent target pursuit as the missile flies over a wide range of aerodynamic variations.

Considering the engagement performance during actual flight, the performance robustness must be examined. Accordingly, homing-loop simulation scenarios for additional flight conditions $FC_i = [V_{mi}$ (Mach), H_{mi} (km), $RMT|_{t=0}$ (km)] with $FC_1 = (1.7, 16.25, 8.0)$, $FC_2 = (2.1, 16.25, 8.0)$, $FC_3 = (1.9, 13.75, 8.0)$, $FC_4 = (2.3, 13.75, 8.0)$, $FC_5 = (1.7, 11.25, 8.0)$, $FC_6 = (2.1, 11.25, 8.0)$, $FC_7 = (1.9, 8.75, 8.0)$, $FC_8 = (2.3, 8.75, 8.0)$ were performed. These cases were not considered in the prescribed GC parameter design. Fig. 13 shows the resultant flight trajectories for the off-designed flight conditions with the previously designed GC parameter set. The averaged final MDs were obtained, respectively, as 3.1, 0.9, 1.7, 0.4, 2.8, 2.0, 3.2, and 2.5 (m). Compared to Fig. 12 the previous design still offers satisfactory engagement performance and the system does not consume much control effort during flight.

VI. Conclusion

This paper proposed a new method for designing the GC parameters of guided missiles. The T–S fuzzy model and gain scheduling were used to synthesize the GC parameters over a complete set of flight conditions. Consequent function parameter design of the fuzzy rules was formulated as a constraint optimization problem with the cost function representing the final miss distance and control energy consumption. A GA was applied to solve the optimization problem and fit multiple constraints due to the homing loop stability requirement and hardware limitations. This novel design approach offers a systematic way to characterize a simple but robust solution that covers a wide range of aerodynamic variations. The efficacy gives it great potential in practical applications.

References

[1] M. Grayson, *Principles of Guided Missile Design*. New York: Van Nostrand, 1960.
[2] E. J. Eichblatt Jr., Ed., *Test and Evaluation of the Tactical Missile*. Washington, DC: AIAA, 1989.
[3] C. F. Lin, *Modern Navigation, Guidance, and Control Processing*. Englewood Cliffs, NJ: Prentice-Hall, 1991.
[4] P. Zarchan, *Tactical and Strategic Missile Guidance*. Washington, DC: AIAA, 1994.
[5] R. Eberhardt and K. A. Wise, "Automated gain schedules for missile autopilots using robustness theory," in *Proc. 1st IEEE Conf. Contr. Applicat.*, Dayton, OH, 1992, pp. 234–250.
[6] D. P. White, J. G. Wozniak, and D. A. Lawrence, "Missile autopilot design using gain scheduling technique," in *Proc. 26th Southeastern Symp. Syst. Theory*, Athens, OH, 1994, pp. 606–610.
[7] C. L. Lin and H. W. Su, "Adaptive fuzzy gain scheduling in guidance system design," *AIAA J. Guid., Contr., Dyna.*, vol. 24, pp. 683–692, 2001.
[8] S. Tan, C. C. Hang, and J. S. Chai, "Gain scheduling: From conventional to neuro-fuzzy," *Automatica*, vol. 33, pp. 411–419, 1997.
[9] T. Takagi and M. Sugeno, "Fuzzy identification of systems and its applications to modeling and control," *IEEE Trans. Syst., Man, Cybern.*, vol. SMC-15, pp. 116–132, 1985.
[10] T. L. Seng, M. B. Khalid, and R. Yusof, "Tuning of a neuro-fuzzy controller by genetic algorithm," *IEEE Trans. Syst., Man, Cybern. B*, vol. 29, pp. 226–236, 1999.
[11] P. Siarry and F. Guely, "A genetic algorithm for optimizing Takagi-Sugeno fuzzy rule bases," *Fuzzy Sets Syst.*, vol. 99, pp. 37–47, 1999.
[12] A. T. de Sousa and M. K. Madrid, "Optimization of Takagi-Sugeno fuzzy controllers using a genetic algorithm," in *Proc. 9th IEEE Int. Conf. Fuzzy Syst.*, San Antonio, TX, 2000, pp. 30–35.
[13] D. Goldberg, *Genetic Algorithms in Search, Optimization and Machine Learning*. Reading, MA: Addison-Wesley, 1989.
[14] R. A. Hull and R. W. Johnson, "Performance enhancement of a missile autopilot via genetic algorithm optimization techniques," in *Proc. Amer. Contr. Conf.*, 1994, pp. 1680–1684.
[15] Y. S. Kim, H. W. G. Han, and T. Y. Kuo, "An intelligent missile autopilot using genetic algorithm," in *Proc. 1997 IEEE Int. Conf. Syst., Man, Cybern*, Orlando, FL, 1997, pp. 1954–1959.

Chun-Liang Lin was born in Tainan, Taiwan, R.O.C., in 1958. He received the Ph.D. degree in aeronautical and astronautical engineering from the National Cheng Kung University, Taiwan, in 1991.

He is currently a Professor in the Department of Automatic Control Engineering, Feng Chia University, Taichung, Taiwan. His research interests include guidance and control, intelligent control, and robust control.

Rei-Min Lai was born in Taichung, Taiwan, R.O.C, in 1977. He received the B.S. degree in electrical engineering and M.S. degree in automatic control engineering from the Feng Chia University, Taichung, Taiwan, in 1999 and 2001, respectively.

His research interests are intelligent control and flight control.